Journal of Applied Polymer Science

Antitumor Efficacy of Doxorubicin Encapsulated Within PEGylated Poly(amidoamine) Dendrimers

Huihui Liao,[1†] Hui Liu,[2†] Yulin Li,[1] Mengen Zhang,[2] Helena Tomás,[1] Mingwu Shen,[2] Xiangyang Shi[1,2]

[1]CQM—Centro de Química da Madeira, Universidade da Madeira, Campus da Penteada 9000-390, Funchal, Portugal

[2]College of Chemistry, Chemical Engineering and Biotechnology, Donghua University, Shanghai 201620, People's Republic of China

Huihui Liao and Hui Liu contributed equally to this work.

Correspondence to: X. Shi (E-mail: xshi@dhu.edu.cn)

ABSTRACT: We report here a general approach to using poly(amidoamine) (PAMAM) dendrimers modified with polyethylene glycol (PEG) as a platform to encapsulate an anticancer drug doxorubicin (DOX) for *in vitro* cancer therapy applications. In this approach, PEGylated PAMAM dendrimers were synthesized by conjugating monomethoxypolyethylene glycol with carboxylic acid end group (*m*PEG-COOH) onto the surface of generation 5 amine-terminated PAMAM dendrimer (G5.NH_2), followed by acetylation of the remaining dendrimer terminal amines. By varying the molar ratios of *m*PEG-COOH/G5.NH_2, G5.NHAc-*m*PEG_n ($n = 5$, 10, 20, and 40, respectively) with different PEGylation degrees were obtained. We show that the PEGylated dendrimers are able to encapsulate DOX with approximately similar loading capacity regardless of the PEGylation degree. The formed dendrimer/DOX complexes are water soluble and stable. *In vitro* release studies show that DOX complexed with the PEGylated dendrimers can be released in a sustained manner. Further cell viability assay in conjunction with cell morphology observation demonstrates that the G5.NHAc-*m*PEG_n/DOX complexes display effective antitumor activity, and the DOX molecules encapsulated within complexes can be internalized into the cell nucleus, similar to the free DOX drug. Findings from this study suggest that PEGylated dendrimers may be used as a general drug carrier to encapsulate various hydrophobic drugs for different therapeutic applications. © 2014 Wiley Periodicals, Inc. J. Appl. Polym. Sci. **2014**, *131*, 40358.

KEYWORDS: dendrimers; hyperbranched polymers and macrocycles; drug delivery systems; nanoparticles; nanowires and nanocrystals

Received 19 November 2013; accepted 27 December 2013

DOI: 10.1002/app.40358

INTRODUCTION

As a notable class of highly branched synthetic macromolecules, dendrimers, especially poly(amidoamine) (PAMAM) dendrimers, possess controllable molecular size, monodispersity, and abundant surface functional groups.[1–4] These features have endowed them with great potential in a wide range of applications from templates or stabilizers for formation of metal nanoparticles,[5–7] drug delivery systems,[8–13] tissue engineering,[14,15] gene transfection[16–18] to molecular imaging applications.[19–26] For biomedical applications, it is essential to neutralize the dendrimer terminal amines in order to avoid the issues of toxicity and nonspecific cell membrane binding. Besides the surface acetylation reaction,[7,27] another most effective strategy to render the dendrimers with good biocompatibility is to modify the dendrimers with polyethylene glycol (PEG). PEG is a nontoxic, nonimmunogenic, and water-soluble polymer that can be covalently conjugated onto the surface of dendrimers to improve the biocompatibility of dendrimers and to effectively increase their bloodstream circulation time.[25,28]

With the great advantage of PEGylation, PEGylated dendrimers have been used in drug delivery applications.[28–30] For instance, antimalarial drug chloroquine phosphate,[29] fluorouracil,[30] or methotrexate[28] can be physically encapsulated within PEGylated dendrimers for different therapeutic applications. The major advantages to use dendrimers as a platform for drug delivery applications are summarized as follows: (1) the highly branched internal cavity of dendrimers can be used for encapsulation of hydrophobic drugs to improve their water solubility; (2) the size of dendrimers is sufficiently small (e.g., the size of generation 5 (G5) PAMAM dendrimers is 5.4 nm), rendering them

Additional Supporting Information may be found in the online version of this article.

© 2014 Wiley Periodicals, Inc.

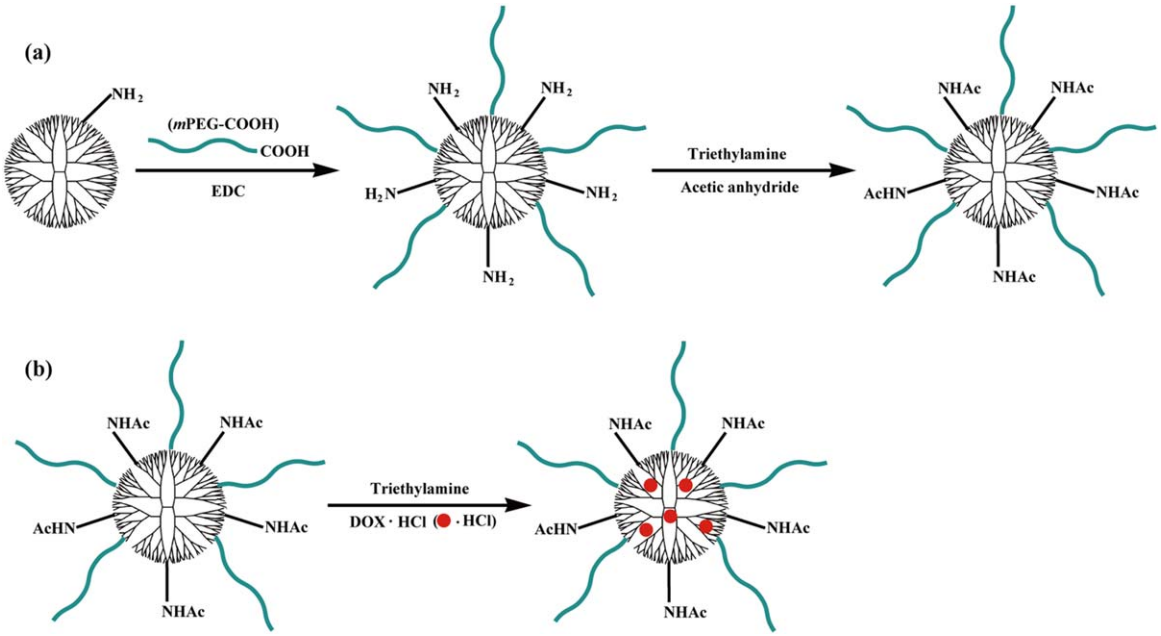

Figure 1. Schematic illustration of the preparation of PEGylated G5 PAMAM dendrimers (a) and the encapsulation of DOX within the dendrimers (b). [Color figure can be viewed in the online issue, which is available at wileyonlinelibrary.com.]

with an ability to pass through the renal filter, and hence, the dendrimers are not required to be degradable; and (3) the surface of dendrimers can be easily modified with targeting ligands, imaging dyes, and drugs to achieve desirable functionalities.[1,11,31–36]

Doxorubicin (DOX) has been commonly used in the treatment of a wide range of cancers, including hematological malignancies, many types of carcinoma, and soft tissue sarcomas. Due to the severe drawbacks of free DOX, such as prominent cytotoxicity to normal cells or tissues, water-insolubility, and easiness to be cleared by the blood stream,[37,38] development of a nanocarrier system to load and release DOX is essential. Various nanoscale delivery systems have been developed to improve the water solubility, bioavailability, and the tumor inhibition efficacy of DOX.[38–42] Among many of the developed drug delivery systems, dendrimers have been used as one of the most attractive carriers to load DOX, either by covalently linking DOX[43–46] on their surface or physically encapsulating or complexing DOX within their interior or onto their surface.[38,47]

In our previous work, we used a multifunctional G5 PAMAM dendrimer-based platform to encapsulate DOX for targeted cancer therapy. We showed that the formed dendrimer/DOX complexes with each dendrimer encapsulating approximately one DOX molecule are water soluble and stable, can release DOX in a sustained manner, and can specifically inhibit the growth of cancer cells.[38] In another work, we have shown that the type of dendrimer surface functional group greatly impacts the anticancer activity of a potential anticancer drug 2-methoxyestradiol (2-ME) encapsulated within the G5 dendrimers, and acetylated G5 dendrimers are able to render the 2-ME drug with noncompromised anticancer activity.[12] These prior work along with the advantage of PEGylation modification of dendrimers leads us to hypothesize that the degree of PEGylation modification may impact the drug encapsulation efficiency and release kinetics, which is crucial for further development of multifunctional PEGylated dendrimer nanoplatforms for targeted cancer therapy.

In this study, we synthesized PEGylated G5 PAMAM dendrimers with the remaining dendrimer terminal amine groups being fully acetylated for DOX delivery applications (Figure 1). By varying the molar ratios of monomethoxypolyethylene glycol with carboxylic acid end group (*m*PEG-COOH)/amine-terminated G5 dendrimer ($G5.NH_2$), G5.NHAc-$mPEG_n$ ($n = 5$, 10, 20, and 40, respectively) with different PEGylation degrees were obtained. The formed PEGylated dendrimers were characterized via ^1H NMR techniques and used as a platform to encapsulate DOX drug. The DOX encapsulation efficiency, release kinetics, and the cell biological evaluation of the dendrimer/DOX complexes were investigated in detail. To the best of our knowledge, this is the first report related to a systematic study of the effect of PEGylation degree on the DOX drug encapsulation efficacy, delivery, and *in vitro* anticancer activity using G5 PAMAM dendrimers as a platform. The results generated from this study may provide a basis for a rational design of functional dendrimer/drug complexes for various therapeutic applications, especially for cancer therapy.

EXPERIMENTAL

Materials

Ethylenediamine core $G5.NH_2$ PAMAM dendrimers with a polydispersity index less than 1.08 were purchased from Dendritech (Midland, MI). 1-(3-Dimethylaminopropyl)−3-ethylcarbodiimide hydrochloride (EDC) was supplied by Aldrich and was used as received. *m*PEG-COOH (Mw 2000) was from Shanghai Yanyi Biotechnology Corporation (Shanghai, China). All other chemicals were obtained from Sigma-Aldrich and used without

further purification. The water used in all the experiments was purified using a Milli-Q Plus 185 water purification system (Millipore, Bedford, MA) with a resistivity higher than 18 MΩ cm. Regenerated cellulose dialysis membranes (molecular weight cutoff, MWCO = 10,000) were acquired from Fisher.

Synthesis of G5.NHAc-*m*PEG$_n$

G5.NH_2 dendrimers were covalently conjugated with *m*PEG-COOH via an EDC coupling reaction, followed by acetylation of dendrimer remaining terminal amines to generate PEGylated G5 dendrimers. The feed molar ratio of *m*PEG-COOH/G5.NH_2 was ranged from 5/1, 10/1, 20/1, to 40/1. Take the feed molar ratio of 10/1 as an example, *m*PEG-COOH (10.0 mg) was dissolved into 5 mL water and then EDC (4.8 mg) of fivefold molar excess over *m*PEG-COOH was added into the above solution to activate the carboxyl group of *m*PEG-COOH. The mixture was reacted under magnetic stirring for 3 h. Then, the EDC-activated *m*PEG-COOH was dropwise added into a G5.NH_2 aqueous solution (13.0 mg, 5 mL) and allowed to react for 3 days at room temperature to get the raw product of G5.NH_2-*m*PEG_{10}. After that, the remaining amines of the dendrimers were converted to acetyl groups by reacting with acetic anhydride according to our previous work.[27,48] In brief, triethylamine (46.4 μL) was added to an aqueous solution of the raw product of G5.NH_2-*m*PEG_{10} under magnetic stirring for 30 min. Then, acetic anhydride (26.2 μL) was added to the above mixture solution while stirring, and the mixture was allowed to react for 24 h. The crude product was extensively dialyzed against phosphate buffered saline (PBS) (three times, 2 L) and water (three times, 2 L) for 3 days to remove the excess of reactants and byproducts, followed by lyophilization to get G5.NHAc-*m*PEG_{10}. G5.NHAc-*m*PEG_5, G5.NHAc-*m*PEG_{20}, and G5.NHAc-*m*PEG_{40} were obtained according to the same procedure. For comparison, nonPEGylated G5 dendrimers (fully acetylated G5 dendrimers, G5.NHAc) were also prepared according to the procedures reported in the literature.[12,48]

Characterization Techniques

UV–vis spectra were collected using a UV–vis spectrophotometer (GBC-Cintra 40, Australia). Samples were dissolved in water before measurements. ^{1}H NMR spectra were recorded using a Bruker Avance II 400 MHz NMR spectrometer. Samples were dissolved in D_2O before measurements. Zeta-potential measurements were carried out using a Zetasizer Nano ZS system (Malvern, UK) equipped with a standard 633 nm laser. All samples with a concentration of 0.5 mg mL^{-1} were measured under different pH conditions (pH 5.0, 7.0, and 10.0, respectively).

Encapsulation of DOX within G5.NHAc-*m*PEG$_n$ Dendrimers

G5.NHAc-*m*PEG_n dendrimers ($n = 5$, 10, 20, 40) (10.0 mg) were dissolved in 3 mL water. Doxorubicin hydrochloride (DOX·HCl) with 10 molar equivalents of the dendrimers was dissolved in 300 μL methanol and was neutralized with 5 μL triethylamine to generate DOX solution, which is insoluble in water. Then, the DOX solution was mixed with the dendrimer aqueous solution under magnetic stirring overnight to allow the evaporation of the methanol solvent. The G5.NHAc-*m*PEG_n/DOX mixture solution was centrifuged (12,000 rpm for 5 min) to remove the precipitates related to noncomplexed free DOX. The precipitate was collected and dissolved into 8 mL methanol for UV–vis analysis. The supernatant was lyophilized to obtain the G5.NHAc-*m*PEG_n/DOX complexes. For comparison, G5.NH_2/DOX and G5.NHAc/DOX complexes were also prepared using the same protocol. By quantifying the noncomplexed free DOX dissolved in methanol via a DOX absorbance (at 480 nm)/concentration calibration curve, the average number of DOX molecules loaded within each dendrimer was able to be estimated by subtracting the initial amount of DOX with the amount of noncomplexed free DOX.

In Vitro Release Kinetic Study

One-milliliter solution of G5.NH_2/DOX, G5.NHAc/DOX, or G5.NHAc-*m*PEG_n/DOX complexes in water was placed in a dialysis bag with MWCO of 10,000, hermetically tied, and suspended in 8 mL of aqueous release medium, PBS buffer (pH 7.4), or acetate buffer (pH 5.0). The entire system was kept in a vapor-bathing constant temperature vibrator at 37°C. The buffer medium (1.5 mL) was taken out at each predetermined time interval and measured by UV–vis spectrophotometer. The volume of the outer phase buffer medium was maintained constant by replenishing the corresponding buffer solution with a volume of 1.5 mL.

Cell Biological Evaluation

HeLa cells (a human cervical carcinoma cell line), chosen as a model cancer cell line, were continuously grown in the cell culture dishes with the Dulbecco's Modified Eagle's Medium supplemented with 10% fetal bovine serum, 100 U/mL penicillin, and 100 U/mL streptomycin. The culture was maintained at 37°C in a wet incubator with 5% CO_2, and the medium was replaced every 3 days.

To check if G5.NHAc-*m*PEG_n/DOX complexes are therapeutically active, a 3-(4.5-dimethylthiazol-2-yl)-2,5-diphenyltetrazolium bromide (MTT) assay was used to quantitatively evaluate the cell viability.[32] One day before the experiments, cells were seeded into a 96-well plate at a density of 8000 cells per well in a complete medium. The next day, the medium was replaced with fresh medium containing free DOX·HCl (2.5 μ*M*), G5.NH_2/DOX, G5.NHAc/DOX, or G5.NHAc-*m*PEG_n/DOX complexes with the same DOX concentration in PBS (20 μL) and then the cells were incubated for 48 h at 37°C. Note that for the DOX encapsulation and release studies, water-insoluble DOX was used; while for cell biological evaluation, water-soluble DOX·HCl was used as a control to check the therapeutic activity of the free drug.

After 48 h incubation with free DOX·HCl, G5.NH_2/DOX, G5.NHAc/DOX, or G5.NHAc-*m*PEG_n/DOX complexes, the metabolic activity of cells was then detected by adding 20 μL MTT solution (5 mg/mL) into each well. After 4 h incubation at 37°C, 200 μL of dimethyl sulfoxide was added to dissolve the formazan crystals. Then, the plates were read at 550 nm using a microplate reader (model Victor^3 1420, PerkinElmer). Mean and standard deviation for the triplicate wells were reported. One way ANOVA statistical analysis was performed to evaluate the significance of the therapeutic efficacy of the DOX drug. 0.05 was selected as the significance level, and the data were indicated with (*) for $P < 0.05$, (**) for $P < 0.001$, and (***) for

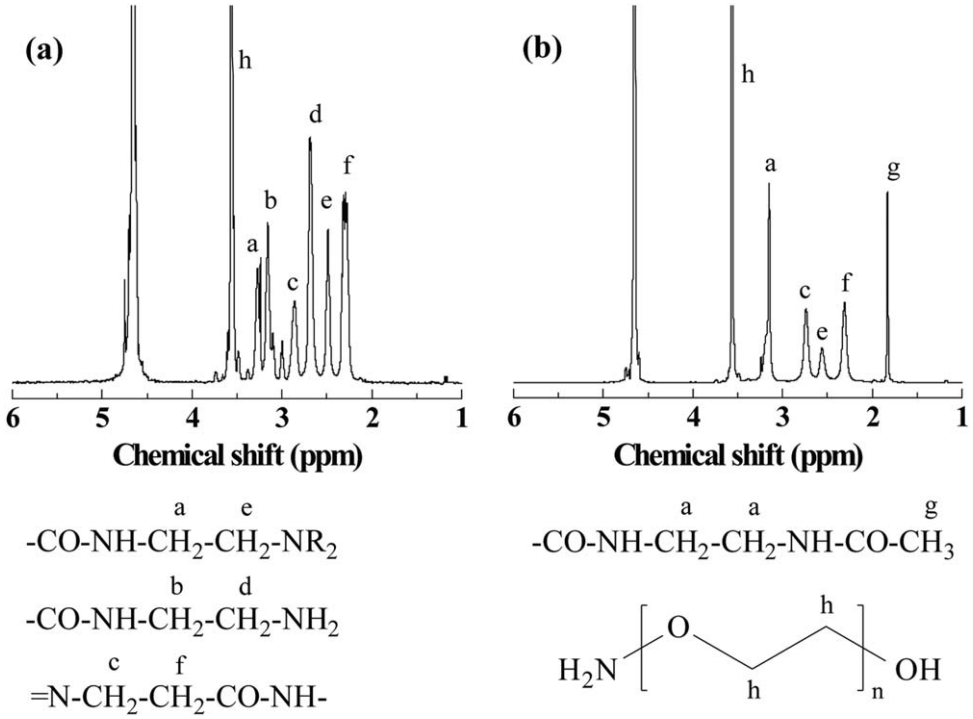

Figure 2. ^{1}H NMR spectra of PEGylated G5 PAMAM dendrimers with *m*PEG/G5.NH$_2$ molar ratio at 10/1 before (a) and after (b) acetylation.

$P < 0.0001$, respectively. After treatment with free DOX·HCl, G5.NH$_2$/DOX, G5.NHAc/DOX, or G5.NHAc-*m*PE G$_n$/DOX complexes, cell morphology was observed by fluorescence microscopy (Nikon Eclipse TE 2000E inverted microscope).

Intracellular DOX Uptake

The intracellular uptake of free DOX·HCl or G5.NHAc-*m*PEG$_n$/DOX complexes was observed by fluorescence microscopy. Briefly, HeLa cells were seeded into a 96-well plate at a density of 8000 cells per well in a complete medium. The next day, the medium was replaced with fresh medium containing free DOX·HCl, G5.NH$_2$/DOX, G5.NHAc/DOX, or G5.NHAc-*m*PEG$_{20}$/DOX complexes with the same DOX concentration (2.5 μM) in PBS (20 μL) and the cells were incubated for 3 h at 37°C. HeLa cells treated with PBS were used as control. Thereafter, the culture medium was removed, and the cells were rinsed three times with PBS and fixed with 3.7% formaldehyde for 10 min. The cell nuclei were counterstained with 4′,6-diamidino-2-phenylindole (DAPI) at room temperature for 10 min. Cell morphology was observed by fluorescence microscopy.

RESULTS AND DISCUSSION

Synthesis of PEGylated G5 PAMAM Dendrimers

Due to their small size (5.4 nm, comparable with hemoglobin) and sufficient terminal functional groups, G5 PAMAM dendrimers were selected as the platform for drug delivery applications. PEGylated G5 PAMAM dendrimers were synthesized by two steps of surface modification reaction [Figure 1(a)]: (1) EDC coupling reaction; and (2) acetylation.

The formed PEGylated G5 PAMAM dendrimers were characterized by ^{1}H NMR spectroscopy. Taken G5.NHAc-*m*PEG$_{10}$ as an example (Figure 2), the *m*PEG proton peaks can be observed at around 3.6 ppm both before [Figure 2(a)] and after [Figure 2(b)] acetylation. The peaks at 2.1–3.4 ppm can be assigned to the —CH$_2$— protons of G5 PAMAM dendrimers. Based on NMR integration, the number of *m*PEG moieties attached onto each dendrimer molecule was calculated to be 6.7. The successful acetylation of the remaining terminal amines of G5.NH$_2$-*m*PEG$_{10}$ dendrimers was also confirmed by ^{1}H NMR spectroscopy [Figure 2(b)]. The emerging peak at 1.87 ppm can be assigned to the —CH$_3$ protons of the acetyl groups, indicating the successful acetylation of the dendrimer terminal amines, in agreement with the literature.[5,27] Via the NMR integration, the practical numbers of *m*PEG moieties attached onto each dendrimer molecule for G5.NHAc-*m*PEG$_5$, G5.NHAc-*m*PEG$_{20}$, and G5.NHAc-*m*PEG$_{40}$ were calculated to be 3.5, 15.0, and 27.8, respectively (Table I).

Encapsulation of DOX within PEGylated G5 PAMAM Dendrimers

The relatively hydrophobic interior of dendrimers enables the effective encapsulation of hydrophobic DOX drug [Figure 1(b)]. The G5.NHAc-*m*PEG$_n$/DOX complexes are expected to improve the water solubility of DOX and thus enhance the DOX bioavailability for biomedical applications. UV–vis spectroscopy was used to characterize the formed G5.NH$_2$/DOX, G5.NHAc/DOX, and G5.NHAc-*m*PEG$_n$/DOX complexes (Figure 3). The UV–vis spectra of DOX dissolved in ethanol and G5.NH$_2$, G5.NHAc, or G5.NHAc-*m*PEG$_n$ ($n = 5$, 10, 20, 40) dendrimers without DOX were also recorded for comparison. It is clear that free DOX shows a strong absorption peak at 481 nm, while all dendrimers without DOX encapsulation do not have absorption features in

Table I. The PEGylation Degree and the Number of DOX Molecules Encapsulated within Each Dendrimer Molecule

Samples	$[N_T]^a$	$[N_A]^b$	$[N_D]^c$
G5.NH_2	0	0	5.5
G5.NHAc	0	0	4.5
G5.NHAc-*m*PEG_5	5	3.5	7.8
G5.NHAc-*m*PEG_{10}	10	6.7	5.4
G5.NHAc-*m*PEG_{20}	20	15.0	5.1
G5.NHAc-*m*PEG_{40}	40	27.8	5.6

[a] Number of *m*PEG attached onto each dendrimer according to the feed molar ratio.
[b] Actual number of *m*PEG attached onto each dendrimer determined by ^{1}H NMR.
[c] Average number of DOX molecules encapsulated within each dendrimer determined by UV–vis spectroscopy.

a wavelength range of 300–800 nm due to the aliphatic nature of dendrimer backbones. The encapsulation of DOX leads to a new absorption peak at 481 nm for G5.NH_2/DOX, G5.NHAc/DOX, and G5.NHAc-*m*PEG_n/DOX complexes under similar dendrimer concentrations. This indicates that DOX has been successfully encapsulated within all the dendrimers. The DOX payload within G5.NH_2, G5.NHAc, and G5.NHAc-*m*PEG_n dendrimers was analyzed with UV–vis spectroscopy. The number of DOX molecules encapsulated within each G5.NH_2, G5.NHAc, G5.NHAc-*m*PEG_5, G5.NHAc-*m*PEG_{10}, G5.NHAc-*m*PEG_{20}, and G5.NHAc-*m*PEG_{40} dendrimer was estimated to be 5.5, 4.5, 7.8, 5.4, 5.1, and 5.6, respectively (Table I). The number of DOX molecules encapsulated within each G5.NHAc-*m*PEG_n dendrimers with different PEGylation degrees appears not to be significantly different. This may be due to the fact that the DOX encapsulation occurs through its interaction with the hydrophobic dendrimer interior, rather than that occurs with the hydrophilic peripheral PEG chains. It should be noted that the

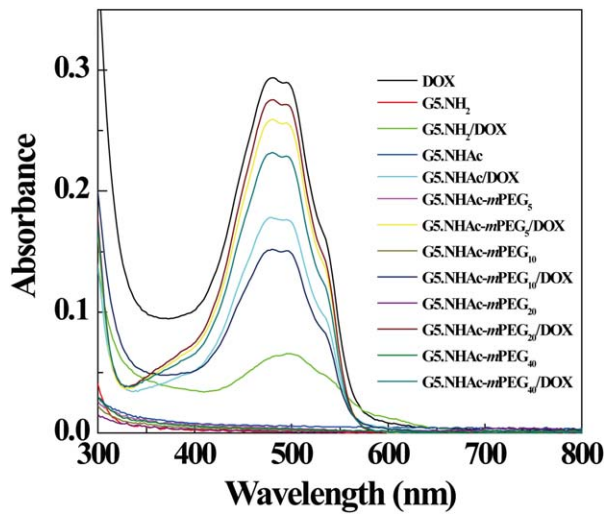

Figure 3. UV–vis spectra of free DOX dissolved in methanol and all the other dendrimers or dendrimer/DOX complexes dissolved in water. [Color figure can be viewed in the online issue, which is available at wileyonlinelibrary.com.]

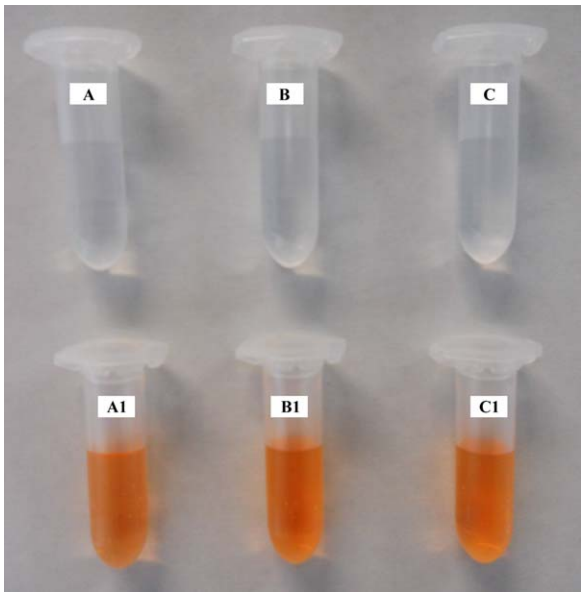

Figure 4. Photographs of the aqueous solutions of G5.NHAc-*m*PEG_{20} dendrimer (A, B, and C) and G5.NHAc-*m*PEG_{20}/DOX complex (A1, B1, and C1) under different pH conditions (pH = 10.0, 7.0, and 5.0 from left to right for both panels). [Color figure can be viewed in the online issue, which is available at wileyonlinelibrary.com.]

number of DOX encapsulated within G5.NHAc dendrimers is 4.5, larger than that encapsulated within acetylated G5 dendrimers modified with folic acid (FA) and fluorescein isothiocyanate (FI) reported in our previous work.[38] This may be because the multifunctional FA- and FI-modified G5 dendrimers have steric hindrance that limits effective DOX loading into the dendrimer interior. Apparently, the hydrophilic PEG chain-induced steric hindrance is not as significant as that induced by the relatively hydrophobic moieties (e.g., FI or FA) attached onto the dendrimer surface.

The stability of the G5.NHAc-*m*PEG_n/DOX complexes is of paramount importance for their biological applications. G5.NHAc-*m*PEG_{20}/DOX was selected as a model to evaluate the stability of the formed complexes. We showed that the lyophilized powders of both G5.NHAc-*m*PEG_{20}/DOX complex and G5.NHAc-*m*PEG_{20} dendrimer without DOX were able to be dissolved in aqueous solution and were stable under different pH conditions (pH = 5.0, 7.0, and 10.0, respectively) for at least 1 month at room temperature (Figure 4). The surface potentials of dendrimer/DOX complexes under different pH conditions are listed in Table II. This information is important for understanding the cellular interactions of the complexes. The larger values at pH 5.0 for each complex compared with those at pH 7.0 and 10.0 should be ascribed to the protonation of a portion of the dendrimer tertiary amines.[49] The changes of the surface potential of the complexes with pH followed the same trend to that described in our previous work.[9,38] In addition, the G5.NHAc-*m*PEG_n/DOX complexes dispersed in different types of aqueous media (e.g., water, PBS, and cell culture medium) stored in 4°C were stable for at least 12 months, which is essential for their further biological applications.

Table II. Zeta Potential Values of All the Dendrimer/DOX Complexes under Different pH Conditions

	Zeta-potential (mV)		
Materials	pH = 10.0	pH = 7.0	pH = 5.0
G5.NH_2/DOX	31.37 ± 0.45	46.33 ± 3.67	49.67 ± 1.40
G5.NHAc/DOX	1.09 ± 0.16	12.80 ± 1.42	15.70 ± 1.91
G5.NHAc-*m*PEG_5/DOX	5.52 ± 0.16	26.67 ± 1.80	29.57 ± 1.62
G5.NHAc-*m*PEG_{10}/DOX	1.46 ± 0.38	12.03 ± 0.21	14.50 ± 0.10
G5.NHAc-*m*PEG_{20}/DOX	3.47 ± 0.42	18.03 ± 2.64	22.23 ± 0.67
G5.NHAc-*m*PEG_{40}/DOX	5.08 ± 0.83	11.20 ± 0.10	14.27 ± 0.25

In Vitro Release Kinetic Studies

To ensure the anticancer therapeutic activity, the encapsulated DOX drug has to be able to be released. The *in vitro* DOX release from the G5.NH_2/DOX, G5.NHAc/DOX, and G5.NHAc-*m*PEG_n/DOX complexes were investigated in PBS (pH = 7.4) or acetate buffer (pH = 5.0) at 37°C. The cumulative release of DOX from the complexes showed that the drug was released in a sustained manner (Figure 5). In contrast, free DOX was quickly released and about 94% was released within just 2 h [Figure 5(a)]. In both buffer media, the release of DOX from the G5.NH_2/DOX, G5.NHAc/DOX, and G5.NHAc-*m*PEG_n/DOX complexes followed a biphasic pattern, which was characterized by an initial faster release, followed by a sustained release. In PBS (pH = 7.4), about 5.4%, 41.4%, 50.2%, 29.1%, 39.8%, and 34.8% of DOX was released within 2 h and about 11.9%, 51.4%, 73.0%, 45.1%, 52.2%, and 52.5% of DOX was released within 48 h from the G5.NH_2, G5.NHAc, G5.NHAc-*m*PEG_5, G5.NHAc-*m*PEG_{10}, G5.NHAc-*m*PEG_{20}, and G5.NHAc-*m*PEG_{40} dendrimer/drug complex, respectively [Figure 5(a)]. For comparison, the drug release rate was decreased in acetate buffer (pH = 5.0). About 3.4%, 21.7%, 31.7%, 12.6%, 22.2%, and 18.8% of DOX was released within 2 h and ~5.5%, 30.3%, 42.3%, 17.1%, 29.5%, and 26.0% of the drug was released within 48 h from the same corresponding dendrimer/drug complex [Figure 5(b)]. The prolonged release of DOX from the complexes under both pH conditions implies that the relatively hydrophobic interior of dendrimer molecules is extremely effective in the retention of the hydrophobic DOX drug. It seems that the DOX release rate does not follow a distinct relationship as a function of the degree of dendrimer PEGylation.

For a typical complex (e.g., G5.NHAc-*m*PEG_{20}/DOX), the release rate of DOX under pH 5.0 was much slower than that under pH 7.4 (Supporting Information Figure S1). This could be due to the fact that hydrogen bonding between the nonprotonated dendrimer terminal amines/dendrimer terminal *m*PEG moieties and DOX plays an important role in regulating the release of DOX from the dendrimer interior. Under an acidic pH condition, the protonated DOX molecules are unlikely able to form strong hydrogen bonding with the dendrimer terminal functional groups (nonprotonated amines and terminal polar C—O—C bonds of PEG moieties), leading to a slower release of DOX. In contrast, under slightly basic condition at pH 7.4, the quite neutralized DOX molecules are able to form strong hydrogen bonding with the dendrimer terminal functional groups, resulting in a faster release rate of DOX from the dendrimer interior. The same explanation can be applied for other dendrimers without PEGylation. In all cases, the much slower release of G5.NH_2/DOX complex may be due to the fact that it is very difficult for the dendrimer terminal amines (protonated under both pH conditions with much higher protonation degree under acidic pH conditions) to form hydrogen bonding with the DOX molecules, thereby preventing the effective release of DOX molecules from the dendrimer interior. Detailed mechanism is still under investigation.

Therapeutic Efficacy of G5.NHAc-*m*PEG_n/DOX Complexes

The therapeutic efficacy of DOX complexed within G5.NH_2, G5.NHAc, and G5.NHAc-*m*PEG_n dendrimers was tested using HeLa cells. After incubation of the respective dendrimer/DOX

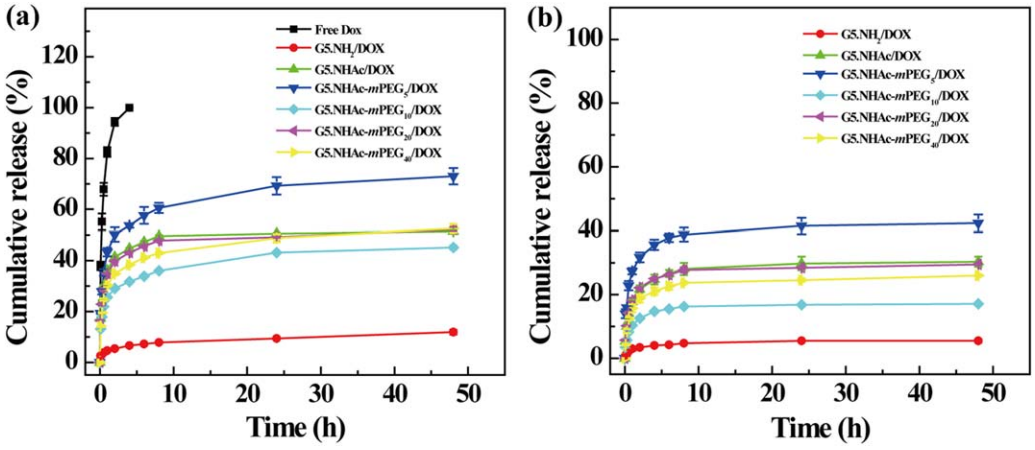

Figure 5. Cumulative release of DOX from G5.NH_2/DOX, G5.NHAc/DOX, and G5.NHAc-*m*PEG_n/DOX complexes in PBS (pH = 7.4) (a) and acetate buffer (pH = 5.0) (b). Free DOX dissolved in methanol was used as control. [Color figure can be viewed in the online issue, which is available at wileyonlinelibrary.com.]

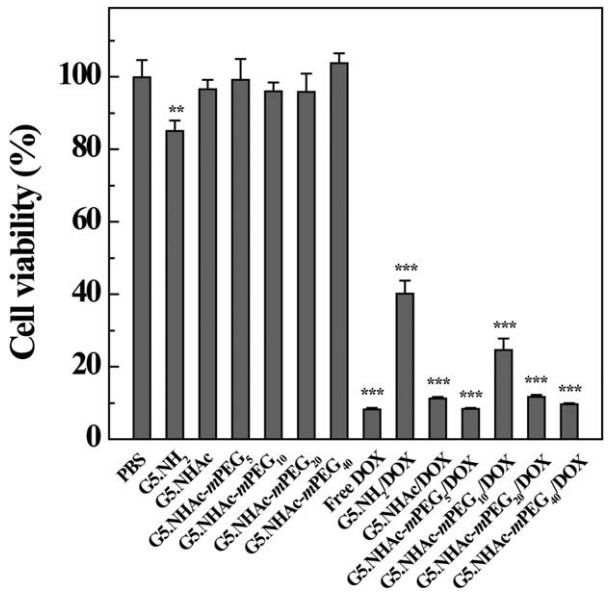

Figure 6. MTT assay of HeLa cell viability after treatment with 20 μL PBS, free DOX·HCl dissolved in 20 μL PBS ([DOX] = 2.5 μM), G5.NH_2/DOX, G5.NHAc/DOX, and G5.NHAc-mPEG$_n$/DOX complexes with DOX concentration of 2.5 μM, and G5.NH_2, G5.NHAc, and G5.NHAc-mPEG$_n$ dendrimers without DOX but with the same dendrimer concentration to those used to encapsulate 2.5 μM DOX, respectively. The data are expressed as mean ± S.D ($n = 3$).

complex with cells for 48 h, an MTT assay was performed to evaluate the cell viability (Figure 6). It appears that similar to free DOX·HCl (2.5 μM), all dendrimer/DOX complexes with DOX concentration of 2.5 μM caused a significant loss of cell viability when compared with the control cells treated with PBS ($P < 0.0001$). To exclude the possible inherent toxicity of the dendrimer carriers, the G5.NH_2, G5.NHAc, and G5.NHAc-mPEG$_n$ ($n = 5$, 10, 20, 40) dendrimers without DOX were also tested with dendrimer concentration similar to that of the corresponding dendrimers used to complex DOX (2.5 μM). It is clear that G5.NHAc and G5.NHAc-mPEG$_n$ dendrimers are nontoxic ($P > 0.05$). In contrast, G5.NH_2 displays toxicity ($P < 0.001$) due to its positive surface charge, in agreement with our previous report.[12] These results suggest that the therapeutic activity of all the dendrimer/DOX complexes (except the G5.NH_2/DOX complex) is solely related to the complexed DOX drug.

The cytotoxicity effect of the dendrimer/DOX complexes was further confirmed by phase contrast microscopic visualization of the cell morphology. Figure 7 shows the morphology of HeLa cells treated with PBS, free DOX·HCl, G5.NH_2/DOX, G5.NHAc/DOX, and G5.NHAc-mPEG$_n$/DOX complexes, respectively. It can be seen that similar to the cells treated with DOX·HCl [Figure 7(b)], all dendrimer/DOX complexes [Figure 7(c–h)] with similar DOX concentration (2.5 μM) induced similar cell morphology changes. A significant portion of the cells became rounded and nonadherent, indicating the apparent cell death. In contrast, no rounded and detached cells can be visualized in cells treated with PBS [Figure 7(a)]. In addition, the HeLa cells were also treated with G5.NH_2, G5.NHAc, or G5.NHAc-mPEG$_n$ dendrimers without the complexation of DOX, but with a dendrimer concentration similar to that of the corresponding dendrimers used for complexation of DOX (2.5 μM). It was found that all dendrimers except G5.NH_2 did not exhibit any prominent toxic effect (Supporting Information Figure S2). This further suggests that the bioactivity of the dendrimer/DOX complexes (except the G5.NH_2/DOX complex) is solely related to the complexed DOX drug. These results corroborate the MTT assay data. It should be noted that from the *in vitro* anticancer activity assay data, the G5.NHAc and PEGylated dendrimers do not show significant differences. However, due to the advantages of PEGylation modification of dendrimers, PEGylated dendrimers should be an ideal nanoplatform for potential practical biomedical applications.

Intracellular DOX Uptake

The therapeutic efficacy of DOX encapsulated within all the dendrimers was further validated by fluorescence imaging of the intracellular DOX uptake (Figure 8). G5.NHAc-mPEG$_{20}$/DOX complex was chosen to compare with dendrimers without mPEG modification. It can be seen that similar to free

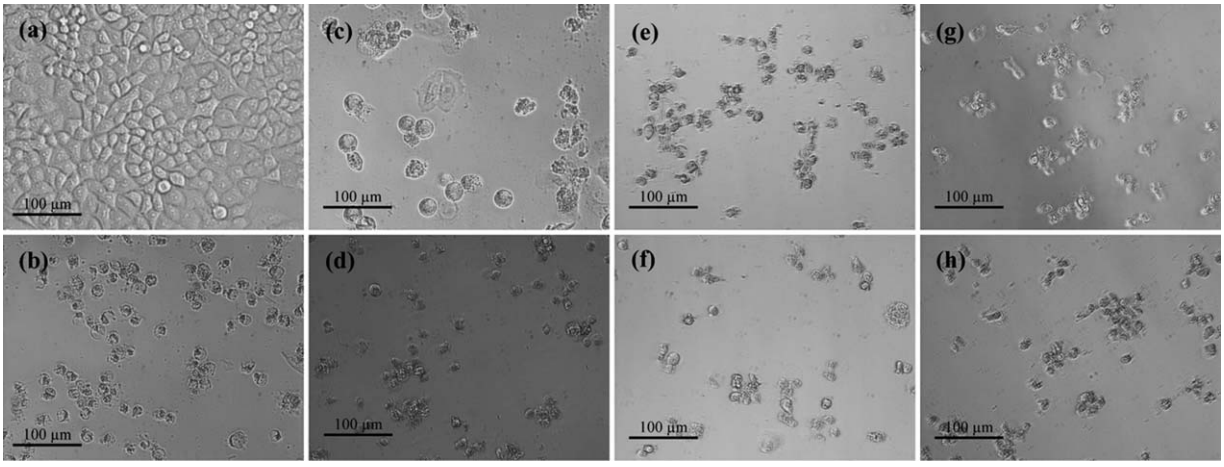

Figure 7. Photomicrographs of the control HeLa cells treated with 20 μL PBS (a), free DOX·HCl (2.5 μM) (b), and DOX (2.5 μM) complexed with G5.NH_2 (c), G5.NHAc (d), and G5.NHAc-mPEG$_n$ ($n = 5$ (e), 10 (f), 20 (g), 40 (h)) dendrimers, respectively.

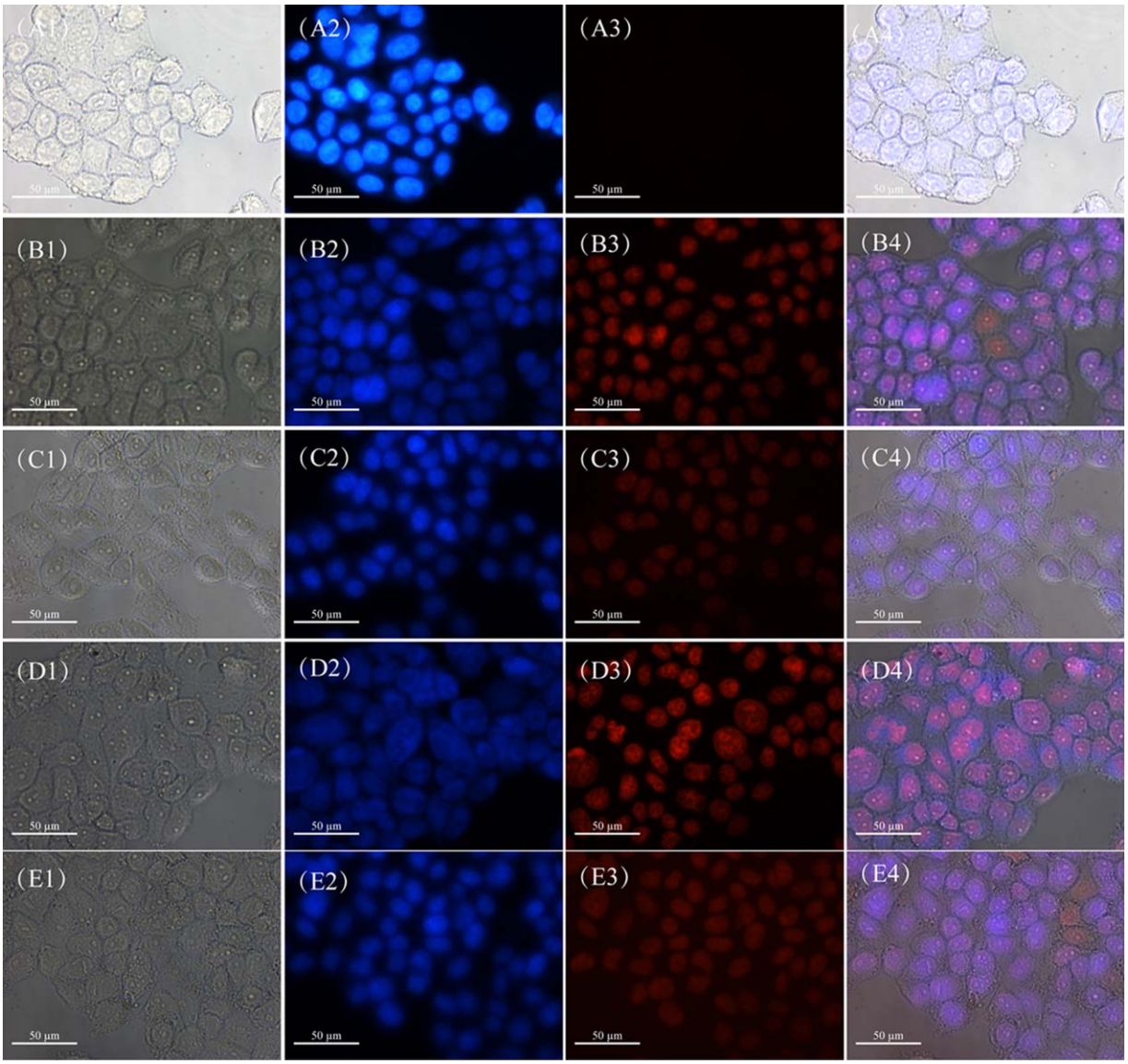

Figure 8. Fluorescence microscopy images of HeLa cells incubated with PBS (A), free DOX·HCl (B), G5.NH_2/DOX (C), G5.NHAc/DOX (D), or G5.NHAc-*m*PEG_{20}/DOX (E) complexes, respectively. In all cases, the DOX concentration was kept at 2.5 μM. For each panel, the images from left to right show bright field, blue fluorescence channel detecting the DAPI dye, red fluorescence channel detecting DOX, and merged images with the above three modes, respectively, under similar instrumental conditions. [Color figure can be viewed in the online issue, which is available at wileyonlinelibrary.com.]

DOX·HCl-treated cells [Figure 8(B)], the red DOX fluorescence signals can be observed in the cell nucleus after 3 h incubation with all the dendrimer/DOX complexes. In contrast, no DOX fluorescence signals were observed in cells treated with PBS. The DOX fluorescence is stronger in the cells incubated with free DOX·HCl, G5.NHAc/DOX, and G5.NHAc-*m*PEG_{20}/DOX complexes than that in cells treated with G5.NH_2/DOX complex. This is because the DOX release from G5.NH_2/DOX complex is much slower than that from other dendrimer/DOX complexes (Figure 5).

CONCLUSION

In summary, we synthesized PEGylated G5 PAMAM dendrimers with different PEGylation degrees for anticancer drug DOX encapsulation and delivery applications. We show that approximately similar numbers of DOX molecules are able to be encapsulated within each PEGylated dendrimer regardless of the dendrimer PEGylation degree. The formed PEGylated dendrimer/DOX complexes are water-soluble, stable, and display a sustained DOX release profile. The DOX release kinetics does not show distinct association with the degree of dendrimer PEGylation. Importantly, the PEGylated dendrimer/DOX complexes are able to effectively inhibit the growth of cancer cells and display desirable therapeutic efficacy, similar to the free DOX drug. With the great advantages of PEGylation modification and the noncompromised anticancer activity of the dendrimer/drug complexes, the developed PEGylated dendrimers may serve as a general nanoplatform for encapsulation and

sustained release of different hydrophobic drugs, thereby affording different biomedical applications.

ACKNOWLEDGMENTS

This research was financially supported by the FCT-Fundação para a Ciência e a Tecnologia (through the projects of PTDC/CTM-NAN/1748/2012, PTDC/CTM-NAN/116788/2010, CQM pluriannual base funding: PEst-OE/QUI/UI0674/2011, and the Portuguese NMR network PTNMR-2013), the Fund of the Science and Technology Commission of Shanghai Municipality (12520705500 for M.S. and 11nm0506400 for X.S.), and the National Natural Science Foundation of China (81341050, 81101150, and 21273032). X.S. gratefully acknowledges the FCT and Santander Bank for the Invited Chair in Nanotechnology. Y.L. thanks the support from FCT via funding through the Science 2008 Program.

REFERENCES

1. Mintzer, M. A.; Grinstaff, M. W. *Chem. Soc. Rev.* **2010**, *40*, 173.
2. Fréchet, J. M. J.; Tomalia, D. A. *Recherche* **2001**, *67*, 02.
3. Esfand, R.; Tomalia, D. A. *Drug Discov. Today* **2001**, *6*, 427.
4. Bronstein, L. M.; Shifrina, Z. B. *Chem. Rev.* **2011**, *111*, 5301.
5. Liu, H.; Wang, H.; Guo, R.; Cao, X.; Zhao, J.; Luo, Y.; Shen, M.; Zhang, G.; Shi, X. *Polym. Chem.* **2010**, *1*, 1677.
6. Shi, X.; Sun, K.; Baker, J. R., Jr. *J. Phys. Chem. C* **2008**, *112*, 8251.
7. Shi, X.; Wang, S. H.; Meshinchi, S.; Van Antwerp, M. E.; Bi, X. D.; Lee, I. H.; Baker, J. R., Jr. *Small* **2007**, *3*, 1245.
8. Wang, Y.; Guo, R.; Cao, X.; Shen, M.; Shi, X. *Biomaterials* **2011**, *32*, 3322.
9. Zhang, M.; Guo, R.; Wang, Y.; Cao, X.; Shen, M.; Shi, X. *Int. J. Nanomed.* **2011**, *6*, 2337.
10. Fox, M. E.; Szoka, F. C.; Fréchet, J. M. *J. Acc. Chem. Res.* **2009**, *42*, 1141.
11. Kukowska-Latallo, J. F.; Candido, K. A.; Cao, Z. Y.; Nigavekar, S. S.; Majoros, I. J.; Thomas, T. P.; Balogh, L. P.; Khan, M. K.; Baker, J. R., Jr. *Cancer Res.* **2005**, *65*, 5317.
12. Shi, X.; Lee, I.; Chen, X. S.; Shen, M. W.; Xiao, S. L.; Zhu, M. F.; Wang, S. H.; Baker, J. R., Jr. *Soft Matter* **2010**, *6*, 2539.
13. Zheng, L. F.; Zhu, J. Y.; Shen, M. W.; Chen, X. S.; Baker, J. R., Jr.; Wang, S. H.; Zhang, G. X.; Shi, X. *Med. Chem. Commun.* **2013**, *4*, 1001.
14. Wathier, M.; Johnson, C. S.; Kim, T.; Grinstaff, M. W. *Bioconjugate Chem.* **2006**, *17*, 873.
15. Khew, S. T.; Yang, Q. J.; Tong, Y. W. *Biomaterials* **2008**, *29*, 3034.
16. Taratula, O.; Garbuzenko, O. B.; Kirkpatrick, P.; Pandya, I.; Savla, R.; Pozharov, V. P.; Minko, T. *J. Controlled Release* **2009**, *140*, 284.
17. Shan, Y.; Luo, T.; Peng, C.; Sheng, R.; Cao, A.; Cao, X.; Shen, M.; Guo, R.; Tomás, H.; Shi, X. *Biomaterials* **2012**, *33*, 3025.
18. Xiao, T.; Hou, W.; Cao, X.; Wen, S.; Shen, M.; Shi, X. *Biomater. Sci.* **2013**, *1*, 1172.
19. Guo, R.; Wang, H.; Peng, C.; Shen, M.; Pan, M.; Cao, X.; Zhang, G.; Shi, X. *J. Phys. Chem. C* **2010**, *114*, 50.
20. Wang, H.; Zheng, L.; Peng, C.; Guo, R.; Shen, M.; Shi, X.; Zhang, G. *Biomaterials* **2011**, *32*, 2979.
21. Chen, Q.; Li, K. A.; Wen, S. H.; Liu, H.; Peng, C.; Cai, H. D.; Shen, M. W.; Zhang, G. X.; Shi, X. *Biomaterials* **2013**, *34*, 5200.
22. Liu, H.; Wang, H.; Guo, R.; Cao, X. Y.; Zhao, J. L.; Luo, Y.; Shen, M. W.; Zhang, G. X.; Shi, X. *Polym. Chem.* **2010**, *1*, 1677.
23. Liu, H.; Xu, Y. H.; Wen, S. H.; Chen, Q.; Zheng, L. F.; Shen, M. W.; Zhao, J. L.; Zhang, G. X.; Shi, X. *Chem. Eur. J.* **2013**, *19*, 6409.
24. Wen, S. H.; Li, K. A.; Cai, H. D.; Chen, Q.; Shen, M. W.; Huang, Y. P.; Peng, C.; Hou, W. X.; Zhu, M. F.; Zhang, G. X.; Shi, X. *Biomaterials* **2012**, *34*, 1570.
25. Peng, C.; Zheng, L. F.; Chen, Q.; Shen, M. W.; Guo, R.; Wang, H.; Cao, X. Y.; Zhang, G. X.; Shi, X. *Biomaterials* **2012**, *33*, 1107.
26. Xiao, T.; Wen, S.; Wang, H.; Liu, H.; Shen, M.; Zhao, J.; Zhang, G.; Shi, X. *J. Mater. Chem. B* **2013**, *1*, 2773.
27. Shi, X.; Lee, I.; Baker, J. R., Jr. *J. Mater. Chem.* **2008**, *18*, 586.
28. Kojima, C.; Kono, K.; Maruyama, K.; Takagishi, T. *Bioconjugate Chem.* **2000**, *11*, 910.
29. Bhadra, D.; Bhadra, S.; Jain, N. K. *Pharm. Res.* **2006**, *23*, 623.
30. Bhadra, D.; Bhadra, S.; Jain, S.; Jain, N. K. *Int. J. Pharm.* **2003**, *257*, 111.
31. Majoros, I. J.; Myc, A.; Thomas, T.; Mehta, C. B.; Baker, J. R. *Biomacromolecules* **2006**, *7*, 572.
32. Majoros, I. J.; Thomas, T. P.; Mehta, C. B.; Baker, J. R. *J. Med. Chem.* **2005**, *48*, 5892.
33. Thomas, T. P.; Choi, S. K.; Li, M.-H.; Kotlyar, A.; Baker, J. R. *Bioorg. Med. Chem. Lett.* **2010**, *20*, 5191.
34. Thomas, T. P.; Huang, B.; Choi, S. K.; Silpe, J. E.; Kotlyar, A.; Desai, A. M.; Zong, H.; Gam, J.; Joice, M.; Baker, J. R., Jr. *Mol. Pharm.* **2012**, *9*, 2669.
35. Thomas, T. P.; Majoros, I. J.; Kotlyar, A.; Kukowska-Latallo, J. F.; Bielinska, A.; Myc, A.; Baker, J. R., Jr. *J. Med. Chem.* **2005**, *48*, 3729.
36. Zhu, J.; Shi, X. *J. Mater. Chem. B* **2013**, *1*, 4199.
37. Patil, R. R.; Guhagarkar, S. A.; Devarajan, P. V. *Crit. Rev. Ther. Drug Carrier Syst.* **2008**, *25*, 1.
38. Wang, Y.; Cao, X.; Guo, R.; Shen, M.; Zhang, M.; Zhu, M.; Shi, X. *Polym. Chem.* **2011**, *2*, 1754.
39. Gabizon, A.; Tzemach, D.; Gorin, J.; Mak, L.; Amitay, Y.; Shmeeda, H.; Zalipsky, S. *Cancer Chemother. Pharmacol.* **2010**, *66*, 43.
40. Meng, H.; Liong, M.; Xia, T.; Li, Z.; Ji, Z.; Zink, J. I.; Nel, A. E. *ACS Nano* **2010**, *4*, 4539.

41. Lai, P. S.; Lou, P. J.; Peng, C. L.; Pai, C. L.; Yen, W. N.; Huang, M. Y.; Young, T. H.; Shieh, M. J. *J. Controlled Release* **2007**, *122*, 39.

42. Kono, K.; Kojima, C.; Hayashi, N.; Nishisaka, E.; Kiura, K.; Watarai, S.; Harada, A. *Biomaterials* **2008**, *29*, 1664.

43. Lee, C. C.; Gillies, E. R.; Fox, M. E.; Guillaudeu, S. J.; Frechet, J. M. J.; Dy, E. E.; Szoka, F. C. *Proc. Natl. Acad. Sci. USA* **2006**, *103*, 16649.

44. De Jesus, O. L. P.; Ihre, H. R.; Gagne, L.; Frechet, J. M. J.; Szoka, F. C. *Bioconjugate Chem.* **2002**, *13*, 453.

45. Zhu, S.; Hong, M.; Tang, G.; Qian, L.; Lin, J.; Jiang, Y.; Pei, Y. *Biomaterials* **2010**, *31*, 1360.

46. Choi, S. K.; Thomas, T.; Li, M.-H.; Kotlyar, A.; Desai, A.; Baker, J. R., Jr. *Chem. Commun.* **2010**, *46*, 2632.

47. Agarwal, A.; Gupta, U.; Asthana, A.; Jain, N. K. *Biomaterials* **2009**, *30*, 3588.

48. Shi, X. Y.; Lesniak, W.; Islam, M. T.; Muniz, M. C.; Balogh, L. P.; Baker, J. R., Jr. *Colloids Surf. A* **2006**, *272*, 139.

49. Cakara, D.; Kleimann, J.; Borkovec, M. *Macromolecules* **2003**, *36*, 4201.